

⁸The model was adjusted so as to agree with observed single-hadron momentum distributions. Limited experimental tests of its predictions for the detailed structure of jets [W. G. Scott, in "Neutrinos—78," edited by Earle C. Fowler (Perdue Univ. Press, to be published)] have proved successful.

⁹The division between configurations of quarks and gluons which give two- and three-jet events is determined by the details of their fragmentation to hadrons. At present the division must be made almost arbitrarily, but our results are not sensitive to the choice (see Ref. 6).

¹⁰If incomplete final states are considered then only a

fraction of the true energy of the event will be measured, so that it is convenient to use the effective H_1/H_0 rather than H_i for this case.

¹¹All processes of $O(g^2)$, including those involving extra initial-state particles (e.g., $\gamma^*Gq \rightarrow q$), must be added in order to obtain an infrared-finite result. To $O(g^2)$, however, only the three-jet parts of $\gamma^*q \rightarrow qG$ and $\gamma^*G \rightarrow q\bar{q}$ contribute to $\langle H_{2l+1} \rangle$ and $\langle H_{2l} \rangle - 1$. $\gamma^*G \rightarrow q\bar{q}$ gives an insignificant contribution.

¹²One may also define two-dimensional analogs of the B_l . These provide an improved formulation of the tests of QCD proposed by H. Georgi and H. D. Politzer, Phys. Rev. Lett. **40**, 3 (1978).

Energy Correlations in Electron-Positron Annihilation: Testing Quantum Chromodynamics

C. Louis Basham, Lowell S. Brown, Stephen D. Ellis, and Sherwin T. Love

Department of Physics, University of Washington, Seattle, Washington 98195

(Received 21 August 1978)

An experimental measure is presented for a precise test of quantum chromodynamics. This measure involves the asymmetry in the energy-weighted opening angles of the jets of hadrons produced in the process $e^+e^- \rightarrow$ hadrons at energy W . It is special for several reasons: It is reliably calculable in asymptotically free perturbation theory; it has rapidly vanishing (order $1/W^2$) corrections due to nonperturbative confinement effects; and it is straightforward to determine experimentally.

Quantum chromodynamics¹ (QCD) is an appealing candidate for the field theory of hadronic interactions, but precise tests are needed to establish its validity. Renormalization-group analyses² show that at large momentum transfer the effective coupling becomes small. This suggests that suitably chosen quantities are precisely calculable at high energies, using "asymptotically free perturbation theory." The central assumption here is that those quantities which are free from infrared mass divergences are reliably calculated at high energies in perturbation theory, using the running coupling constant which vanishes at infinite energy.³ This requires, of course, that energies are well away from (new particle) thresholds (e.g., charm) and that nonperturbative confinement effects are negligible.

The major experimental tests of QCD have been of a semiquantitative nature, involving deeply inelastic lepton scattering from nuclear targets.⁴ In general, such analyses suffer from the necessity of introducing arbitrary functions to describe the constituent distributions within the hadronic target. Electron-positron annihilation avoids such ambiguities since there are no hadrons in the initial state, and various features of this an-

nihilation process have been suggested⁵ as possible precise tests of QCD. Such features must satisfy several criteria in order to be useful: (1) They must exhibit characteristic properties of QCD, e.g., the presence of both fermions and gauge vector bosons or the vanishing of the running coupling as the energy increases [see Eq. (3)]. (2) They must be reliably calculable. This requires freedom from infrared singularities and insensitivity to nonperturbative effects so as to allow a perturbative analysis. (3) They must be accessible to experiment. This constraint argues against studying quantities which are small effects on much larger backgrounds and quantities which are sensitive to the absence of complete (i.e., all particle) data for each annihilation event.

We have previously suggested⁶ the study of the hadronic energy pattern, the "antenna pattern," produced in e^+e^- annihilation as a possible means to test QCD precisely. The experimental quantity to be measured is the hadronic energy radiated into an element of solid angle $d\Omega$ (in direction \hat{r}) divided by the incident energy per unit area in the e^+e^- beams. In terms of the partial cross section for the process $e^+e^- \rightarrow N$ hadrons at

total energy W , the energy pattern cross section is given by

$$\frac{d\Sigma}{d\Omega} = \sum_{N=2}^{\infty} \int \sum_{a=1}^N E_a^{-1} d^3p_a \frac{d^N\sigma}{E_1^{-1}d^3p_1 \cdots E_N^{-1}d^3p_N} S_N \left[\sum_{b=1}^N \frac{E_b}{W} \delta(\Omega_b - \Omega) \right]. \tag{1}$$

(Here S_N represents the factorials necessary to avoid multiple counting of identical particles.) Energy conservation guarantees that the integral of the energy cross section is the usual total cross section. The inclusive energy summation in the energy cross section should render its perturbative formulation free (to all orders) of collinear infrared singularities. The energy weighting should remove those singularities which arise from soft gluon emission.

It should be emphasized that the measurement of the energy cross section, Eq. (1), *does not require any detailed event-by-event analysis* as is the case for tests which specify a quantity involving the definition of a jet axis in each event.⁵

The order- g^2 result for the energy cross section corresponds to the graphs shown in Fig. 1. This result is indeed free of mass singularities. Assuming unpolarized electron-positron beams with total energy W , the energy cross section takes the form⁶

$$\frac{d\Sigma}{d\Omega} = \frac{\alpha^2}{4W^2} \sum_f 3Q_f^2 \left[\left(1 + \frac{\bar{g}_W^2}{4\pi^2} \right) (1 + \cos^2\theta) + \frac{\bar{g}_W^2}{4\pi^2} (1 - 3\cos^2\theta) \right]. \tag{2}$$

Here α is the fine-structure constant ($\sim 1/137$), Q_f is the electric charge of a specific quark type (flavor), and θ is the angle between the direction \hat{r} of the detected energy and the beam direction \hat{l} , $\cos\theta = \hat{r} \cdot \hat{l}$. The asymptotic behavior of the running coupling is given by

$$\bar{g}_W^2 \approx \frac{8\pi^2}{\left[11 - \frac{2}{3}N_f \right] \ln(W/\mu)}, \tag{3}$$

where N_f is the number of quark flavors, and μ is the one-dimensional parameter introduced into the theory via the renormalization-group analysis. It is taken to have a value 500 MeV in order to minimize⁷ the $O(1/\ln^2W)$ corrections to Eq. (3). Experimentally, the important feature of the perturbative energy cross section (2) is the broadening of the lowest-order $1 + \cos^2\theta$ pattern due to hard gluon emission. Nonperturbative confinement effects distribute the energy carried by the

quark and gluons among the observed hadrons. These confinement effects further broaden the distribution. They can be treated phenomenologically⁶ by assuming that the fragmentation of the quarks (produced with a $1 + \cos^2\theta$ distribution) into hadrons occurs with a distribution characterized by a strong cutoff in momentum transverse to the quark direction. These effects produce a contribution to the coefficient of the $1 - 3\cos^2\theta$ term in Eq. (2) of order $\langle h_{\perp} \rangle / W$, where $\langle h_{\perp} \rangle$ is the average transverse momentum in a quark fragmentation jet. At presently available energies the two contributions to this coefficient are of comparable magnitude, but the confinement

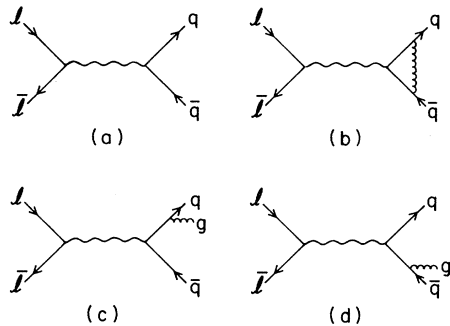


FIG. 1. (a) Lowest-order Feynman graph for $e^+e^- \rightarrow \gamma \rightarrow q\bar{q}$. (b) Vertex modification (wave-function renormalization not shown). (c), (d) Lowest-order gluon emission graphs.

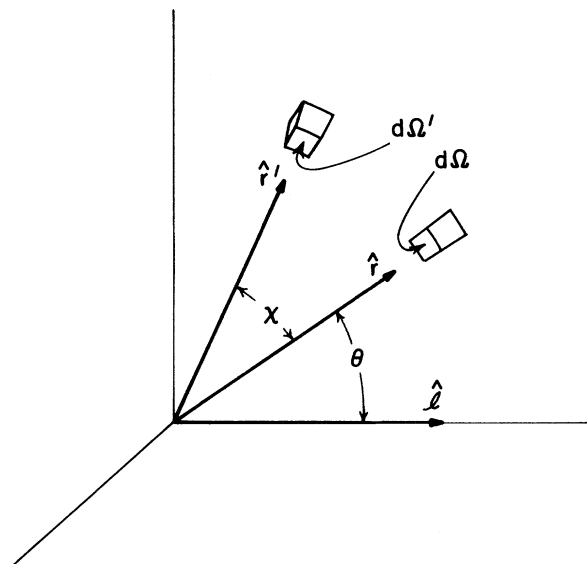


FIG. 2. Geometry for the experiment.

correction vanishes more rapidly with increasing energy than does the perturbative contribution.

The total cross section, σ_{tot} , and the "antenna pattern," $d\Sigma/d\Omega$, form the first two members of a hierarchy of cross sections that probe the details of QCD with increasing precision. The differential cross sections involve *energy weightings* so as to avoid the mass singularities arising from soft and collinear particle production, and thus are amenable to the asymptotically free perturbation analysis. We have studied⁸ the third member of this hierarchy, the energy-energy

correlation cross section. It would be measured, for example, in an experiment employing two calorimeters, one of solid angle $d\Omega$ (in direction \hat{r}), the other of solid angle $d\Omega'$ (in direction \hat{r}') with an angle χ between the directions of the two detectors ($\cos\chi = \hat{r} \cdot \hat{r}'$). This configuration is illustrated in Fig. 2. In each event the energies observed in the two calorimeters are multiplied together and divided by W^2 . This product is then summed over all events. The resulting sum is normalized by the total e^+e^- flux. The energy-energy correlation function is given by

$$\frac{d^2\Sigma}{d\Omega d\Omega'} = \sum_{N=2}^{\infty} \int \prod_{a=1}^N E_a^{-1} d^3p_a \frac{d^N\sigma}{E_1^{-1} d^3p_1 \cdots E_N^{-1} d^3p_N} S_N \left[\sum_{b,c=1}^N \frac{E_b E_c}{W^2} \delta(\Omega_b - \Omega) \delta(\Omega_c - \Omega') \right]. \quad (4)$$

Note that we must use "transparent" calorimeters so that the $b=c$ terms are included. This is necessary to remove collinear divergences. Indeed, by including these terms, energy conservation guarantees that the integral of Eq. (5) over $d\Omega'$ yields the energy pattern, Eq. (1), which is free of infrared divergences (at least to order g^2). In order g^2 and for $|\cos\chi = \hat{r} \cdot \hat{r}'| < 1$, the correlation cross section arises entirely from the gluon emission process of Figs. 1(c) and 1(d). Defining $\xi = \frac{1}{2}(1 - \cos\chi)$ and an azimuthal angle between the planes formed by \hat{r}, \hat{r}' , and \hat{r}, \hat{l} , such that $\cos\varphi = (\hat{l} \times \hat{r}) \cdot (\hat{r}' \times \hat{r}') / (|\hat{l} \times \hat{r}| |\hat{r}' \times \hat{r}'|)^{1/2}$ (cf. Fig. 2), the perturbative calculation yields

$$\begin{aligned} \frac{d^2\Sigma}{d\Omega d\Omega'} = & \frac{\alpha^2}{4W^2} \sum_f 3Q_f^2 \frac{\bar{g}_W^2}{3\pi^2} \frac{1}{32\pi} \frac{1}{1-\xi} \left\{ \left[\left(\frac{36}{\xi^5} - \frac{96}{\xi^4} + \frac{72}{\xi^3} - \frac{16}{\xi^2} \right) \ln(1-\xi) + \frac{36}{\xi^4} - \frac{78}{\xi^3} + \frac{36}{\xi^2} \right] (1 + \cos^2\theta) \right. \\ & + 4\xi(1-\xi) \left[\left(\frac{6}{\xi^5} - \frac{8}{\xi^4} \right) \ln(1-\xi) + \frac{6}{\xi^4} - \frac{5}{\xi^3} - \frac{2}{\xi^2} \right] [\cos^2\varphi - \cos^2\theta (1 + \cos^2\varphi)] \\ & \left. + 2[\xi(1-\xi)]^{1/2} \left[\left(-\frac{36}{\xi^5} + \frac{72}{\xi^4} - \frac{40}{\xi^3} \right) \ln(1-\xi) - \frac{36}{\xi^4} + \frac{54}{\xi^3} - \frac{16}{\xi^2} - \frac{8}{\xi} \right] \cos\theta \sin\theta \cos\varphi \right\}. \quad (5) \end{aligned}$$

For coincident calorimeters ($\cos\chi = 1$) one must include the δ -function contributions arising from the "transparent" calorimeter definition discussed above. For $\cos\chi = -1$, these δ -function contributions arising from the simple quark-antiquark final state corrected by virtual gluon exchange [Figs. 1(a) and 1(b)]. When appropriately regulated, the singular behavior present in Eq. (5) precisely cancels⁸ the δ -function terms in a distribution sense (i.e., when integrated over small angular regions). Thus the energy-energy correlation cross section is divergence free and reliably calculable, at least to second order.

As in the case of the energy pattern, there are nonperturbative (quark fragmentation) contributions of order $\langle h_{\perp} \rangle / W$ to the double-differential energy cross section (4). These corrections have a dependence on the angles θ and φ similar to that of the perturbative result (5) which simply reflects the spin information carried by the virtual photon. However, the dependence of the nonperturbative contribution on χ , the angle between the two energy detectors, is quite different from that in Eq. (5). This difference is made most apparent by choosing $\theta = 90^\circ$ or by integrating over φ . In either case the cross term proportional to $\cos\theta \sin\theta \cos\varphi$ drops out. The φ integrated cross section can be written generally as

$$\int d\varphi \frac{d^2\Sigma}{d\Omega d\Omega'} = \sigma_{\text{tot}} \frac{\bar{g}_W^2}{4\pi^2} \frac{3}{16\pi} [A(\xi) + \cos^2\theta B(\xi)]. \quad (6)$$

The leading $\langle h_{\perp} \rangle / W$ nonperturbative contributions to A and B are even under the interchange $\chi \leftrightarrow \pi - \chi$

($\xi \leftrightarrow 1 - \xi$), while the perturbative QCD form

$$A(\xi) = \frac{1}{6(1-\xi)} \left[\left(\frac{18}{\xi^5} - \frac{42}{\xi^4} + \frac{22}{\xi^3} \right) \ln(1-\xi) + \frac{18}{\xi^4} - \frac{33}{\xi^3} + \frac{7}{\xi^2} + \frac{3}{\xi} + 2 \right], \quad (7a)$$

$$B(\xi) = \frac{1}{6(1-\xi)} \left[\left(\frac{18}{\xi^5} - \frac{66}{\xi^4} + \frac{78}{\xi^3} - \frac{32}{\xi^2} \right) \ln(1-\xi) + \frac{18}{\xi^4} - \frac{57}{\xi^3} + \frac{51}{\xi^2} - \frac{9}{\xi} - 6 \right], \quad (7b)$$

are quite asymmetric about $\chi = \frac{1}{2}\pi$ ($\xi = \frac{1}{2}$), as is illustrated in Fig. 3(a). Thus, as the energy increases, the perturbative QCD contributions (7) dominate the differences

$$D_A(\xi) = A(1-\xi) - A(\xi), \quad (8a)$$

$$D_B(\xi) = B(1-\xi) - B(\xi), \quad (8b)$$

with the nonperturbative corrections being of or-

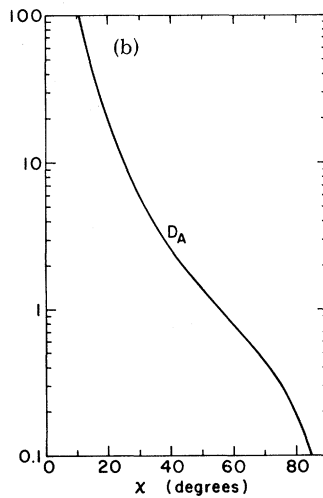
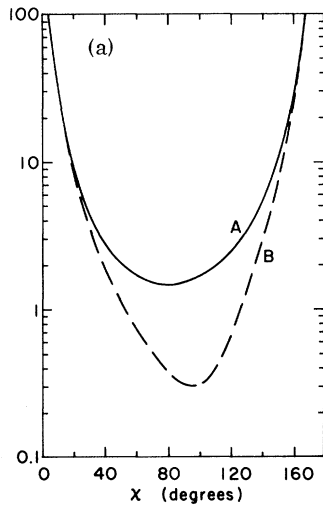


FIG. 3. (a) A and B defined by Eq. (7) as functions of χ . (b) The difference D_A defined by Eq. (8a) as a function of χ .

der $1/W^2$. As an illustration of the size of these perturbative QCD differences, D_A is plotted in Fig. 3(b). Clearly it is large for $\chi \leq 50^\circ$; e.g., the difference is 40% of the sum at $\chi = 35^\circ$.

In actual experiments, it will probably be convenient both to integrate over φ , increasing the counting rate, and to choose $\theta = 90^\circ$, which allows the φ integral to be performed over the largest range in χ without intersecting the beam pipe. In this case only D_A is measured, cf. Eq. (6). We estimate that with reasonable angular bins ($\Delta\theta \approx \Delta\chi \approx \pm 5^\circ$), such measurements of the difference D_A should be quite feasible for the projected intensities of the next generation of e^+e^- machines.

We conclude that the differences, Eq. (8), are measures that satisfy the three criteria presented at the beginning of this Letter. Their experimental determination would constitute a precise test of quantum chromodynamics.

We thank J. E. Rothberg and R. W. Williams for useful conversations. Our work was supported in part by the U. S. Department of Energy.

¹A review appears in W. Marciano and H. Pagels, Phys. Rep. **36C**, 137 (1978).

²D. Gross and F. Wilczek, Phys. Rev. Lett. **26**, 1343 (1973); H. D. Politzer, Phys. Rev. Lett. **26**, 1346 (1973).

³This approach was first suggested by G. Sterman and S. Weinberg, Phys. Rev. Lett. **39**, 1436 (1977).

⁴See, e.g., the reviews by K. Schultze, L. N. Hand, and O. Nachtmann, in *Proceedings of the International Symposium on Lepton and Photon Interactions at High Energies, Hamburg, Germany, 1977*, edited by F. Gutbrod (DESY, Hamburg, Germany, 1977).

⁵H. Georgi and M. Machacek, Phys. Rev. Lett. **39**, 1237 (1977); E. Fahri, Phys. Rev. Lett. **39**, 1587 (1977); A. De Rújula, J. Ellis, E. G. Floratos, and M. K. Gaillard, Nucl. Phys. **B138**, 387 (1978); S. S. Shei, unpublished; S.-Y. Pi, R. Jaffe, and F. Low, Phys. Rev. Lett. **41**, 142 (1978).

⁶C. L. Basham, L. S. Brown, S. D. Ellis, and S. T. Love, Phys. Rev. D **17**, 2298 (1978).

⁷See, e.g., A. De Rújula, H. Georgi, and H. D. Politzer, Ann. Phys. (N.Y.) **103**, 315 (1977).

⁸C. L. Basham, L. S. Brown, S. D. Ellis, and S. T. Love, unpublished.